Application of radial basis functions to evolution equations arising in image segmentation*

Li Shu-Ling(李淑玲)† and Li Xiao-Lin(李小林)

College of Mathematics Science, Chongqing Normal University, Chongqing 400047, *China*

(Received 9 May 2013; revised manuscript received 13 July 2013; published online 10 December 2013)

In this paper, radial basis functions are used to obtain the solution of evolution equations which appear in variational level set method based image segmentation. In this method, radial basis functions are used to interpolate the implicit level set function of the evolution equation with a high level of accuracy and smoothness. Then, the original initial value problem is discretized into an interpolation problem. Accordingly, the evolution equation is converted into a set of coupled ordinary differential equations, and a smooth evolution can be retained. Compared with finite difference scheme based level set approaches, the complex and costly re-initialization procedure is unnecessary. Numerical examples are also given to show the efficiency of the method.

Keywords: radial basis functions, evolution equations, image segmentation, re-initialization

PACS: 87.57.nm **DOI:** 10.1088/1674-1056/23/2/028702

1. Introduction

Image segmentation is a significant branch of image processing and computer vision applications. The aim of segmentation is to separate image domain into a collection of distinct areas, in which other high-level tasks, such as tracking and object recognition, can be further implemented. During the past two decades, the level set method[1] has been widely used in the field of image segmentation and other scientific and engineering problems.[2–9] This is a versatile and simple method of calculating and analyzing the motion of an interface and following the evolution of the interface. The primary idea is to implicitly represent an interface of codimensional one as the zero level set of a function in higher dimension, which is referred to as a level set function, and then derive an evolution equation of the level set function by minimizing a certain energy functional defined at the level set function.[6]

The evolution equation is a time-dependent differential equation and is numerically solved by finite difference methods (FDMs) in most cases. Although these numerical methods have been used to gain accurate solutions, they are often time consuming and computationally expensive. More importantly, in using conventional level set methods, the upwind scheme is usually used to maintain numerical stability, and the level set function often develops irregularities during its evolution, which causes numerical errors and eventually destroys the numerical stability. To accurately solve the evolution equation using FDMs, a numerical remedy procedure called re-initialization[10] is introduced periodically to restore the regularity of the level set function and remain as a stable level set evolution. In re-initialization algorithms, complicated differential equation solving procedures are involved in general. Besides, re-initialization may incorrectly move the zero level set away from its original position.[10] Although alternative techniques without re-initialization were recently developed,[11–13] they often require dedicated and complicated extension of the speed function defined in the zero level set.

Radial basis functions (RBFs) are a class of functions where the Euclidean distance of a fixed node from a variable field point is used as the independent variable. From 1990, RBFs have been used as meshless (or meshfree) methods[14–17] to approximate the solutions of partial differential equations (PDEs).[18–22] The so-called Kansa's method is one of the collocation methods,[18] in which the approximate solution is obtained by collocation with RBFs on nodes.

In recent years, Wang *et al.*[23] developed RBFs-based collocation method for evolution equations arising from the level set-based structural topology optimization. Xie and Mirmehdi[24] presented a research in level set representation and evolution using RBFs. In their work, PDE-based level set evolution equations were used to represent the considered problem, and multiquadric (MQ) function was used to define the implicit level set function. Since MQ is a conditionally positive-definite RBF, the implementation of their methods requires the addition of a polynomial term together with some homogeneous constraint conditions in order to obtain invertible interpolation matrices. As a result, the number of unknowns is added. In addition, Gelas *et al.*[25] explored the use of compactly support radial basis functions (CSRBFs) for the level set evolution equation. Nevertheless, as pointed out by Zhang and Liu,[21] CSRBFs are less accurate than non-

*Project supported by the National Natural Science Foundation of China (Grant No. 11101454), the Educational Commission Foundation of Chongqing City, China (Grant No. KJ130626), and the Program of Innovation Team Project in University of Chongqing City, China (Grant No. KJTD201308).

†Corresponding author. E-mail: shuling1124@163.com

© 2014 Chinese Physical Society and IOP Publishing Ltd

compact RBFs.

In this paper, positive-definite and non-compact RBFs are developed for solving evolution equations appearing in image segmentation. The variational level set evolution equation is used to define the image segmentation problem. Following Refs. [23]–[25], the implicit level set function is interpolated using RBF implicit modeling. Then, by collocation, the original variational level set evolution equation is discretized into a system of mathematically more convenient ordinary differential equations (ODEs). Finally, Euler's method is employed to solve these coupled ODEs. Because the used RBFs are global-support and positive-definite, a smooth level set evolution can be kept without re-initialization. Consequently, the interface contour can be initialized anywhere in the image. Besides, we demonstrate that the segmentation can be implemented even without any initial interface contours.

The rest of this paper is organized as follows. In Section 2 the RBFs interpolation scheme is described. In Section 3, the variational level set evolution equation for image segmentation is presented. Then, a detailed numerical implementation for the evolution equation is provided in the next section. In Section 5 some numerical results are given. Finally, the conclusions are drawn from the present study in Section 6.

2. Radial basis function interpolation

Let Ω be a bounded domain in $\mathbb{R}^2$. A general point of $\mathbb{R}^2$ is denoted by $\boldsymbol{x} = (x, y)$. Assume that there are N distinct nodes $\boldsymbol{x}_j$ $(j = 1, 2, \ldots, N)$ inside the domain Ω.

The radial basis function interpolating $\mu(\boldsymbol{x})$ from the surrounding nodes of a sampling point $\boldsymbol{x}$ can be written as

$$\mu(\boldsymbol{x}) = \sum_{i=1}^{N} a_i R_i(\boldsymbol{x}) = \boldsymbol{R}^{\mathrm{T}}(\boldsymbol{x})\,\boldsymbol{a}, \tag{1}$$

where $R_i(\boldsymbol{x})$ is an RBF, a_i is a coefficient,

$$\boldsymbol{R}^{\mathrm{T}}(\boldsymbol{x}) = [R_1(\boldsymbol{x}), R_2(\boldsymbol{x}), \ldots, R_N(\boldsymbol{x})],$$

and

$$\boldsymbol{a} = [a_1,\ a_2,\ \ldots,\ a_N]^{\mathrm{T}}.$$

The unknown coefficient a_i is normally solved via collocation,

$$\sum_{i=1}^{N} a_i R_i(\boldsymbol{x}_j) = \mu(\boldsymbol{x}_j), \quad j = 1, 2, \ldots, N. \tag{2}$$

The system of Eq. (2) is uniquely solvable providing that the coefficient matrix

$$\boldsymbol{\Psi} = \begin{bmatrix} R_1(\boldsymbol{x}_1) & R_2(\boldsymbol{x}_1) & \cdots & R_N(\boldsymbol{x}_1) \\ R_1(\boldsymbol{x}_2) & R_2(\boldsymbol{x}_2) & \cdots & R_N(\boldsymbol{x}_2) \\ \vdots & \vdots & \ddots & \vdots \\ R_1(\boldsymbol{x}_N) & R_2(\boldsymbol{x}_N) & \cdots & R_N(\boldsymbol{x}_N) \end{bmatrix} \tag{3}$$

is nonsingular. Theoretically, the positive definiteness of the matrix is sufficient to guarantee its invertibility. Nevertheless, most of the globally defined RBFs are only conditionally positive-definite.[21]

The effectiveness and accuracy of the interpolation depend on the choice of RBFs. A variety of RBFs have been suggested and can be employed for this purpose. Three commonly used RBFs are multiquadric (MQ), Gaussian, and thin plate spline (TPS). For MQ and TPS, the linear polynomial basis is required. Gaussian can be implemented without any additional polynomial terms as it is positive-definite.[26] The following Gaussian is chosen in this research:

$$R_i(\boldsymbol{x}) = \mathrm{e}^{-br_i^2}, \tag{4}$$

where b is a shape parameter and $r_i = \|\boldsymbol{x} - \boldsymbol{x}_i\|$ is the Euclidean distance between the interpolation point $\boldsymbol{x}$ and a node $\boldsymbol{x}_i$.

Equation (2) can be expressed in matrix form as follows:

$$\boldsymbol{\Psi} a = \bar{\boldsymbol{\mu}}, \tag{5}$$

where $\bar{\boldsymbol{\mu}} = [\mu(\boldsymbol{x}_1), \mu(\boldsymbol{x}_2), \ldots, \mu(\boldsymbol{x}_N)]^{\mathrm{T}}$. Therefore, the unknown vector $\boldsymbol{a}$ can be obtained uniquely from Eq. (5) as

$$\boldsymbol{a} = \boldsymbol{\Psi}^{-1}\bar{\boldsymbol{\mu}}. \tag{6}$$

Then inserting Eq. (6) into Eq. (1) yields

$$\mu(\boldsymbol{x}) = \boldsymbol{R}^{\mathrm{T}}(\boldsymbol{x})\,\boldsymbol{\Psi}^{-1}\bar{\boldsymbol{\mu}}, \tag{7}$$

where $\boldsymbol{R}^{\mathrm{T}}(\boldsymbol{x})\,\boldsymbol{\Psi}^{-1}$ is the shape function vector.

3. Evolution equation for image segmentation

3.1. Evolution equation

Let $I : \Omega \to \mathbb{R}$ be a prescribed image, then $I(\boldsymbol{x})$ will be the corresponding pixel intensity. The image segmentation problem is to find a contour $\mathcal{C}$ which segments the image domain Ω into two non-overlapping regions Ω_1 and Ω_2. Here, Ω_1 and Ω_2 denote, respectively, the object and the background, and $\mathcal{C}$ is a closed interface boundary between Ω_1 and Ω_2.

In the level set formulation, the embedded interface $\mathcal{C}$ is expressed implicitly by the zeros of a Lipschitz continuous level set function $\phi(\boldsymbol{x})$. Namely, the location of the interface corresponds to the following zero level set

$$\mathcal{C} = \left\{\boldsymbol{x} \in \mathbb{R}^2 \,|\, \phi(\boldsymbol{x}) = 0\right\}.$$

Besides, $\phi(\boldsymbol{x})$ can be used to define Ω_1 and Ω_2 as follows:

$$\begin{cases} \phi(\boldsymbol{x}) = 0, & \forall \boldsymbol{x} \in \mathcal{C}, \\ \phi(\boldsymbol{x}) > 0, & \forall \boldsymbol{x} \in \Omega_1, \\ \phi(\boldsymbol{x}) < 0, & \forall \boldsymbol{x} \in \Omega_2. \end{cases}$$

In order to let the level set function $\phi(\boldsymbol{x})$ dynamically change in time, a continuous speed function V is introduced. Then,

the general form of the evolution of ϕ can be described as the following Cauchy problem:[2]

$$\frac{\partial \phi(\boldsymbol{x},t)}{\partial t} + V(\boldsymbol{x},t)\,\delta_\varepsilon(\phi(\boldsymbol{x},t)) = 0, \tag{8}$$

$$\phi(\boldsymbol{x},0) = \phi_0(\boldsymbol{x}). \tag{9}$$

Equation (8) is referred to as a variational level set evolution equation. Here, t is the artificial time and δ_ε is a regularized Dirac function,[6]

$$\delta_\varepsilon(\phi) = \frac{\varepsilon}{\pi(\varepsilon^2+\phi^2)},$$

where ε is a real positive constant. Besides, $\phi_0(\boldsymbol{x})$ embeds initial position of the interface. In practical computations, the initialization can be obtained either from a priori knowledge about the image to be segmented or from user interaction.[25]

In the traditional level set approaches, the solving procedure of the aforementioned Cauchy problem requires suitable selection of the upwind schemes and re-initialization algorithms. This procedure involves excessive computational efforts and, therefore, restricts the application of the level set approaches.

In the current research, the level set function is to be approximated by RBFs. Then, RBFs implicit model discretizes the aforementioned Cauchy problem into a set of mathematically more convenient coupled ODEs. Thus, the obtained level set function is global smoothness. More importantly, the complex and costly re-initialization is unnecessary on account of the global smoothness. The restriction on the time-step size may be relaxed and the computational efficiency may be increased. In what follows, this developed method is to be discussed in detail.

3.2. The *C–V* model

The level set evolution equation (8) can be derived by minimizing a certain energy functional defined on the level set,[11] such as the Mumford–Shah model,[7] the *C–V* model,[6] the piecewise smoothing model,[8] the local binary fitting model,[9] etc. The *C–V* model is one of the most popular used models, which has been successfully used in segmentation of the image into regions with piecewise constant intensity.

Taking the *C–V* model for example, we set up a framework for the application of RBFs in image segmentation. In the *C–V* level set model, the energy functional is defined by[6]

$$\begin{aligned}&\mathcal{F}(c_1(\phi),c_2(\phi),\phi)\\ &= \gamma\int_\Omega \delta_\varepsilon(\phi)\,\|\nabla\phi\|\,\mathrm{d}\boldsymbol{x}\\ &\quad+\lambda_1\int_\Omega (I(\boldsymbol{x})-c_1(\phi))^2 H(\phi)\,\mathrm{d}\boldsymbol{x}\\ &\quad+\lambda_2\int_{\Omega_2} (I(\boldsymbol{x})-c_2(\phi))^2 (1-H(\phi))\,\mathrm{d}\boldsymbol{x},\end{aligned} \tag{10}$$

where $\gamma \geq 0$, $\lambda_1 > 0$, and $\lambda_2 > 0$ are fixed parameters; $H(\phi)$ is the following regularized Heaviside function,[6]

$$H_\varepsilon(\phi) = \frac{1}{2}\left[1+\frac{2}{\pi}\arctan\left(\frac{\phi}{\varepsilon}\right)\right].$$

Besides, $c_1(\phi)$ and $c_2(\phi)$ are the following constants that approximate, respectively, the image intensities inside and outside the interface $\mathcal{C}$:

$$c_1(\phi) = \frac{\int_\Omega I(\boldsymbol{x})H(\phi)\,\mathrm{d}\boldsymbol{x}}{\int_\Omega H(\phi)\,\mathrm{d}\boldsymbol{x}}$$

and

$$c_2(\phi) = \frac{\int_\Omega I(\boldsymbol{x})(1-H(\phi))\,\mathrm{d}\boldsymbol{x}}{\int_\Omega (1-H(\phi))\,\mathrm{d}\boldsymbol{x}}.$$

Minimizing the energy functional $\mathcal{F}$ with the steepest descent method, the following variational formulation is obtained for the solution of the level set method:[6]

$$\begin{aligned}\frac{\partial\phi}{\partial t} &= \delta_\varepsilon(\phi)\left[\gamma\,\mathrm{div}\left(\frac{\nabla\phi}{\|\nabla\phi\|}\right)-\lambda_1(I(\boldsymbol{x})-c_1(\phi))^2\right.\\ &\quad\left.+\lambda_2(I(\boldsymbol{x})-c_2(\phi))^2\right].\end{aligned}$$

In Eq. (10), the first term on the right-hand side minimizes the length of the interface $\mathcal{C}$ given by the zero-crossing of the level set function $\phi(\boldsymbol{x})$, while the last two terms minimize the gray value variances inside $\mathcal{C}$ and outside $\mathcal{C}$ in two separated phases. Since the approximate function generated by RBFs is intrinsic global smoothness, the smoothness term of the energy functional $\mathcal{F}$ is not required and we set $\gamma = 0$. In addition, because λ_1 and λ_2 govern the tradeoff between the last two terms, we set $\lambda_1 = \lambda_2 = 1$. As a result, the speed function V used in our study is finally represented as

$$V(\boldsymbol{x},t) = (I(\boldsymbol{x})-c_2(\phi))^2 - (I(\boldsymbol{x})-c_1(\phi))^2.$$

4. Numerical solution of the evolution equation

Because the evolution equation (8) is time-dependent, following Refs. [23]–[25], it is assumed that the space and time in the level set function $\phi(\boldsymbol{x},t)$ are separable. Consequently, the RBF interpolation of the level set function $\phi(\boldsymbol{x},t)$ becomes time-dependent as

$$\phi(\boldsymbol{x},t) = \sum_{i=1}^{N} R_i(\boldsymbol{x})\,a_i(t) = \boldsymbol{R}^{\mathrm{T}}(\boldsymbol{x})\,\boldsymbol{a}(t), \tag{11}$$

where $\boldsymbol{a}(t) = [a_1(t), a_2(t), \ldots, a_N(t)]^{\mathrm{T}}$. Inserting Eq. (11) into Eq. (8) yields

$$\sum_{i=1}^{N} R_i(\boldsymbol{x})\frac{\mathrm{d}a_i(t)}{\mathrm{d}t} + V(\boldsymbol{x},t)\,\delta_\varepsilon\left(\sum_{i=1}^{N} R_i(\boldsymbol{x})\,a_i(t)\right) = 0.$$

Then by simple collocations at internal nodes $\boldsymbol{x}_j$, we obtain a set of ODEs

$$\sum_{i=1}^{N} R_i(\boldsymbol{x}_j)\frac{\mathrm{d}a_i(t)}{\mathrm{d}t} + V(\boldsymbol{x}_j,t)\,\delta_\varepsilon\left(\sum_{i=1}^{N} R_i(\boldsymbol{x}_j)\,a_i(t)\right) = 0,$$

$$j = 1, 2, \ldots, N. \tag{12}$$

It is assembled in matrix form as follows:

$$\boldsymbol{\Psi} \frac{\mathrm{d}\boldsymbol{a}(t)}{\mathrm{d}t} + \boldsymbol{F}(t, \boldsymbol{a}(t)) = 0, \tag{13}$$

where $\boldsymbol{\Psi}$ is a known $N \times N$ interpolation matrix given in Eq. (3), $\boldsymbol{a}(t)$ is an unknown vector, and

$$\boldsymbol{F}(t, \boldsymbol{a}(t)) = [F_1, F_2, \ldots, F_N]^{\mathrm{T}}$$

is a vector with

$$F_j = V(\boldsymbol{x}_j, t)\, \delta_\varepsilon \left(\sum_{i=1}^{N} R_i(\boldsymbol{x}_j)\, a_i(t) \right), \quad j = 1, 2, \ldots, N.$$

The resolution of Eq. (13) requires the definition of an initial value for the time-dependent variable $\boldsymbol{a}(t)$. At the initial time $t_0 = 0$, collocating Eq. (11) at internal nodes $\boldsymbol{x}_j$ and using Eq. (9) lead to

$$\boldsymbol{\Psi} a(0) = \boldsymbol{\Phi}_0,$$

where $\boldsymbol{\Phi}_0 = [\phi_0(\boldsymbol{x}_1), \phi_0(\boldsymbol{x}_2), \ldots, \phi_0(\boldsymbol{x}_N)]^{\mathrm{T}}$ is a known vector. Therefore, the initial value is

$$\boldsymbol{a}(t_0) = \boldsymbol{a}(0) = \boldsymbol{\Psi}^{-1} \boldsymbol{\Phi}_0. \tag{14}$$

Now, the level set evolution equation (8) is converted into a set of coupled nonlinear ODEs of Eq. (13). Thus, the original time-dependent initial value problem defined by Eqs. (8) and (9) in the traditional level set methods is reduced into a time-dependent interpolation problem for the initial values of the unknown variable $\boldsymbol{a}(t)$, and the evolution of the level set is governed by the time-dependent coupled equation (13) with initial value given by Eq. (14).

Since the stiffness matrix $\boldsymbol{\Psi}$ is theoretically invertible, equation (13) can be rewritten as

$$\frac{\mathrm{d}\boldsymbol{a}(t)}{\mathrm{d}t} = -\boldsymbol{\Psi}^{-1} \boldsymbol{F}(t, \boldsymbol{a}(t)).$$

Then, using the first-order forward Euler's method leads to

$$\boldsymbol{a}(t_{n+1}) = \boldsymbol{a}(t_n) - \tau \boldsymbol{\Psi}^{-1} \boldsymbol{F}(t_n, \boldsymbol{a}(t_n)), \quad n = 0, 1, 2, \ldots, \tag{15}$$

where $\tau > 0$ is the time-step size. Experimentally, we observe that the segmentation remains unchanged when $\tau \in [0.1, 10]$. This result shows the robustness of the current method to the selection of the time-step size. Therefore, τ is fixed to be 1 for the following experiments.

Equation (15) involves the inverse of the matrix $\boldsymbol{\Psi}$. Since the distance is directionless, we have $R_i(\boldsymbol{x}_j) = R_j(\boldsymbol{x}_i)$, which implies that the coefficient matrix $\boldsymbol{\Psi}$ is symmetric. Besides, the coefficient matrix is positive-definite. Therefore, as done in Ref. [25], the Cholesky decomposition is used to avoid computing $\boldsymbol{\Psi}^{-1}$. At the initial stage, $\boldsymbol{\Psi}$ is decomposed as the product of a lower triangular matrix $\boldsymbol{L}$ and its transpose; that is,

$$\boldsymbol{\Psi} = \boldsymbol{L}\boldsymbol{L}^{\mathrm{T}}.$$

Then, for each iteration we solve instead of Eq. (15) the following lower triangular system

$$\boldsymbol{L}\boldsymbol{u}_{n+1} = \boldsymbol{F}(t_n, \boldsymbol{a}(t_n)),$$

and upper triangular system

$$\boldsymbol{L}^{\mathrm{T}} \boldsymbol{v}_{n+1} = \boldsymbol{u}_{n+1}.$$

Finally, equation (15) is equivalent to

$$\boldsymbol{a}(t_{n+1}) = \boldsymbol{a}(t_n) - \tau \boldsymbol{v}_{n+1}. \tag{16}$$

With standard arguments used in the proof of Proposition 1 in Ref. [25], we can prove that in Eq. (15) the norm of the unknown vector $\boldsymbol{a}(t)$ can increase slowly at each iteration step. To bound it, the following normalization is added after Eq. (16) for each iteration

$$\boldsymbol{a}(t_{n+1}) = \frac{\boldsymbol{a}(t_{n+1})}{\|\boldsymbol{a}(t_{n+1})\|}. \tag{17}$$

Because equation (11) indicates that equation (17) simply corresponds to $\phi / \|\boldsymbol{a}(t_{n+1})\|$ and the division of the level set function $\phi(\boldsymbol{x}, t)$ by a nonzero coefficient does not change its associated interface, this normalization makes sense. As in Ref. [25], a global convergence of the algorithm is obtained if the following condition is satisfied:

$$\|\boldsymbol{a}(t_n) - \boldsymbol{a}(t_{n-1})\| \leq \|\boldsymbol{a}(t_{n-1}) - \boldsymbol{a}(t_{n-2})\|.$$

5. Numerical experiments

Firstly, we apply the present method to an image shown in Fig. 1. In this analysis, the RBF centers are located on a regular rectangular grid with 77×59 nodes. To show the advantage of the current RBF-based collocation method, we also apply the CSRBF-based collocation method[25] and the well-known C–V model using finite difference scheme with re-initialization procedure[6] to this image.

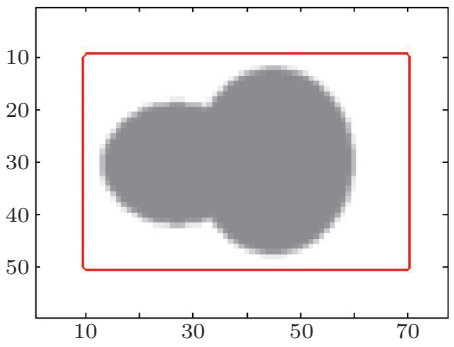


Fig. 1. (color online) An image to be segmented (the solid line denotes the initial contour).

Figure 2 shows the comparison among the behaviors of the level set evolution in the three formulations. The initial level set is computed from the region enclosed by the quadrilateral enclosing as shown in Fig. 1. In this case, our RBF method takes 15.17 s with 3 iterations, the CSRBF method takes 17.59 s with 9 iterations, while the *C*–*V* model takes 244.8 s with 2500 iterations. From this figure, it can be found that both our RBF method and the CSRBF method achieve convergent and accurate results, but only roughly accurate result is obtained for the *C*–*V* model. Therefore, our RBF method is faster than both the CSRBF method and the *C*–*V* model for this image.

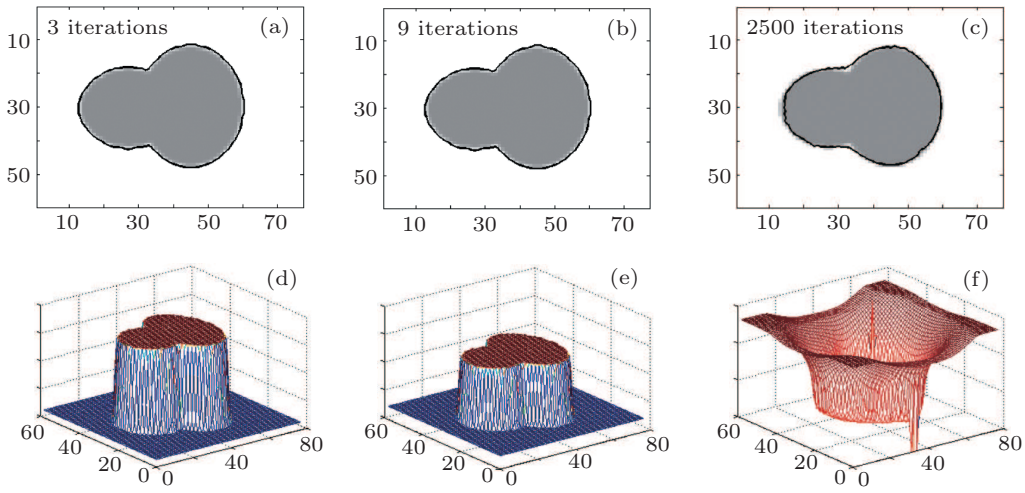


Fig. 2. (color online) Segmentation results with initial interface contour shown in Fig. 1. Panels (a)–(c) show the zero level contours obtained from our RBF method, the CSRBF method, and the *C*–*V* model, respectively. Panels (d)–(f) display the converged level set functions of our RBF method, the CSRBF method, and the *C*–*V* model, respectively.

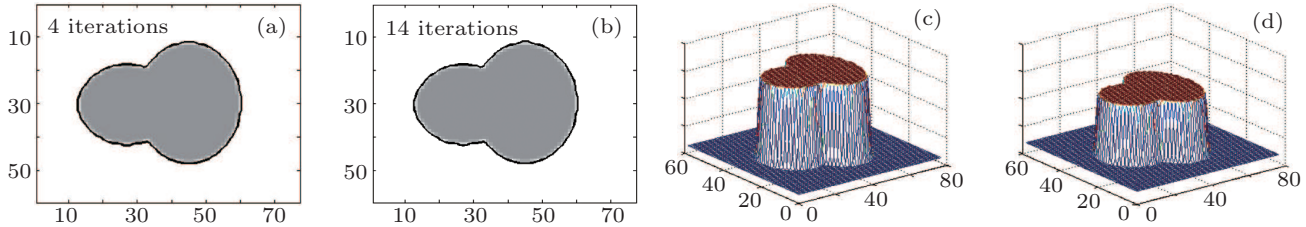


Fig. 3. (color online) Segmentation results without any initial interface contour. Panels (a) and (b) shows the zero level contours obtained from our RBF method and the CSRBF method, respectively. Panels (d) and (f) exhibit the converged level set functions obtained from our RBF method and the CSRBF method, respectively.

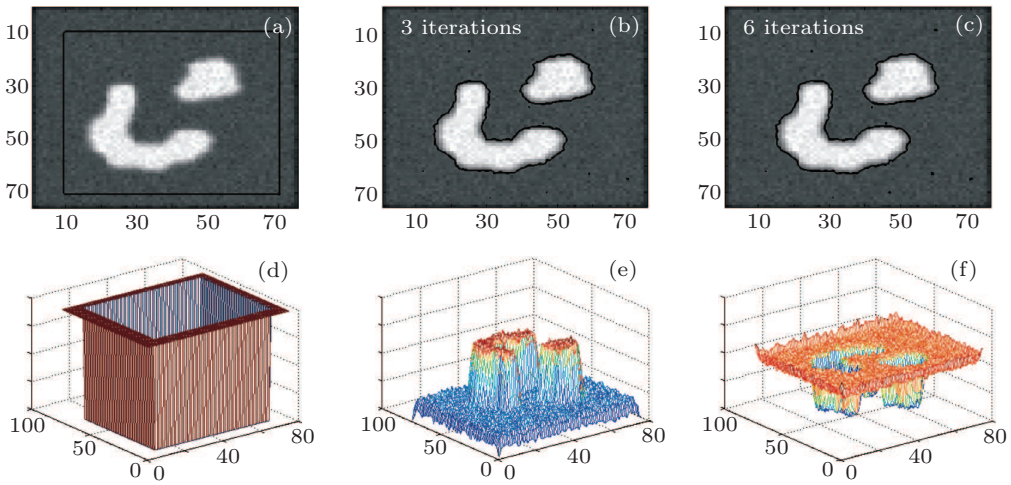


Fig. 4. (color online) Segmentation results on a noisy image. Panels (a)–(c) show the zero level contours of the initial interface contour, the zero level contours obtained from our RBF method and the CSRBF method, respectively. Panel (d) exhibits the level set function of the initial interface contour. Panels (e) and (f) display the converged level set functions obtained from our RBF method and the CSRBF method, respectively.

When the initial interface contour is absent, figure 3 shows the results obtained from our RBF method and the CSRBF method. In this case, our RBF method takes 15.59 s with 4 iterations, while the CSRBF method takes 20.08 s with 14 iterations. This figure indicates that the segmentation can be implemented even without any initial interface contour.

Next, figure 4 shows the segmentation results on a noisy image with weak boundaries. In this analysis, the RBF centers are located on a regular rectangular grid with 75×75 nodes. The initial level set is computed from the region enclosed by the quadrilateral enclosing, as shown in Fig. 4(a). In this case, our RBF method takes 28.17 s with 3 iterations, while the CSRBF method takes 29.50 s with 6 iterations. Again, both our RBF method and the CSRBF method achieve convergent and accurate results, and our RBF method is faster than the CSRBF method for this model.

6. Conclusions

An RBF-based collocation method for image segmentation using variational level set evolution equations is presented in this paper. The implicit level set function is approximated by using the RBF implicit modeling. Because of the global smoothness of this representation, a high level of accuracy and smoothness of the implicit function is achieved. Besides, the evolution equation is discretized into a mathematically more convenient coupled ODE system and the original time-dependent initial value problem becomes a relatively simple time-dependent interpolation problem. It turns out that a relatively smooth level set evolution can be maintained without re-initialization due to the use of RBFs.

Numerical experiments are conducted to validate the current RBF-based collocation method. For all examples, a convergent solution is gained. The numerical experiments also indicate that the developed RBF-based collocation method is faster than both the CSRBF-based collocation method and the *C–V* model using finite difference scheme with re-initialization procedure. Consequently, the developed algorithm is attractive for evolution equations in image segmentation.

References

[1] Osher S and Sethian J 1988 *J. Comput. Phys.* **78** 12
[2] Tsai R and Osher S 2003 *Commun. Math. Sci.* **1** 120
[3] Osher S and Fedkiw RP 2001 *J. Comput. Phys.* **169** 463
[4] Ma J F, Hou K, Bao S L and Chen C 2011 *Chin. Phys. B* **20** 028701
[5] Zhao G Z 2010 *Chin. Phys. B* **19** 070203
[6] Chan T and Vese L 2001 *IEEE T. Image Process.* **10** 266
[7] Mumford D and Shah J 1989 *Commun. Pure Appl. Math.* **42** 577
[8] Vese L and Chan T 2002 *Int. J. Comput. Vis.* **50** 271
[9] Caselles V, Catte F, Coll T and Dibos F 1993 *Numer. Math.* **66** 1
[10] Sethian J 1999 *Level Set Methods and Fast Marching Methods* (Cambridg: Cambridge University Press)
[11] Li C M 2005 *Proc. IEEE Conf. Comput. Vis. Pattern Recogn.* **1** 430
[12] Li C M, Xu C Y, Gui C F and Fox M D 2010 *IEEE T. Image Process.* **19** 154
[13] Zhang K, Zhang L, Song H and Zhang D 2013 *IEEE T. Image Process.* **22** 258
[14] Cheng R J and Cheng Y M 2007 *Acta Phys. Sin.* **56** 5569 (in Chinese)
[15] Chen Li and Cheng Y M 2008 *Acta Phys. Sin.* **57** 6047 (in Chinese)
[16] Ren H P, Cheng Y M and Zhang W 2009 *Chin. Phys. B* **18** 4065
[17] Li X L and Li S L 2013 *Chin. Phys. B* **22** 080204
[18] Kansa E J 1990 *Comput. Math. Appl.* **19** 147
[19] Li X L, Zhu J L and Zhang S G 2011 *Appl. Math. Model.* **35** 737
[20] Li X L, Zhu J L and Zhang S G 2009 *Eng. Anal. Bound. Elem.* **33** 1273
[21] Zhang X and Liu Y 2004 *Meshless Methods* (Beijing: Tsinghua University Press) pp. 43–48 (in Chinese)
[22] Dai B D and Cheng Y M 2007 *Acta Phys. Sin.* **56** 597 (in Chinese)
[23] Wang S, Lim K, Khoo B and Wang M 2007 *J. Comput. Phys.* **221** 395
[24] Xie X and Mirmehdi M 2011 *Image Vision Comput.* **29** 167
[25] Gelas A, Bernard O, Friboulet D and Prost R 2007 *IEEE T. Image Process.* **16** 1873
[26] Powell M J D 1997 *Advances in Numerical Analysis* (Oxford: Oxford Science Publications)